Biochimica et Biophysica Acta 1848 (2015) 1032–1040

Contents lists available at ScienceDirect

Biochimica et Biophysica Acta

journal homepage: www.elsevier.com/locate/bbamem

The organization of melatonin in lipid membranes

Hannah Dies, Bonnie Cheung, Jennifer Tang, Maikel C. Rheinstädter *

Department of Physics and Astronomy, McMaster University, Hamilton, Ontario Canada

ARTICLE INFO

Article history:
Received 2 August 2014
Received in revised form 29 December 2014
Accepted 10 January 2015
Available online 17 January 2015

Keywords:
Melatonin
Lipid membrane
Molecular structure
Molecular organization
Melatonin-enriched domain
X-ray diffraction

ABSTRACT

Melatonin is a hormone that has been shown to have protective effects in several diseases that are associated with cholesterol dysregulation, including cardiovascular disease, Alzheimer's disease, and certain types of cancers. We studied the interaction of melatonin with model membranes made of dimyristoylphosphatidylcholine (DMPC) at melatonin concentrations ranging from 0.5 mol% to 30 mol%. From 2-dimensional X-ray diffraction measurements, we find that melatonin induces a re-ordering of the lipid membrane that is strongly dependent on the melatonin concentration. At low melatonin concentrations, we observe the presence of melatonin-enriched patches in the membrane, which are significantly thinner than the lipid bilayer. The melatonin molecules were found to align parallel to the lipid tails in these patches. At high melatonin concentrations of 30 mol%, we observe a highly ordered melatonin structure that is uniform throughout the membrane, where the melatonin molecules align parallel to the bilayers and one melatonin molecule associates with 2 lipid molecules. Understanding the organization and interactions of melatonin in membranes, and how these are dependent on the concentration, may shed light into its anti-amyloidogenic, antioxidative and photoprotective properties and help develop a structural basis for these properties.

1. Introduction

The interactions of proteins and small molecules with lipid membranes play a large role in maintaining the integrity and functionality of the cell membrane, and significant changes in these interactions are involved in the pathology of many diseases [1]. Melatonin is a hormone that is produced in the central nervous system by the pineal gland for circadian cycle regulation. However, it has also been shown to be produced by several peripheral tissues, which suggests that it may have other physiological roles [2]. Melatonin has been of recent interest in the study of membrane/small molecule interactions; it acts as an antioxidant, may be preventative against cardiovascular disease and may also inhibit the formation of toxic amyloid structures [3,4].

While cholesterol, which is speculated to be correlated to an increased risk for Alzheimer's disease, leads to a decrease in membrane fluidity, melatonin is a largely hydrophilic amino acid derivative hormone, which has been shown to reside in the head group region [5], increasing membrane fluidity and causing a corresponding increase in head group area and a decrease in bilayer thickness [5–7]. Increased fluidification of the membranes is speculated to inhibit peptide insertion, as the amyloid peptide has been found to preferably interact with gel phase membranes [8].

Although cholesterol and melatonin are highly integrated into the biochemical pathways of the cell, previous studies have identified that their mechanism of influence is at least in part structural; many of their effects are as a result of biophysical interactions that influence the protein and membrane structure [6,9,10]. Choi et al. have recently shown through Langmuir–Blodgett methods and molecular dynamics simulations that melatonin is able to offset the rigidifying effects of cholesterol in dipalmitoylphosphatidylcholine (DPPC) monolayers [11]. Additionally, Saija et al. have suggested that melatonin's fluidifying action may lead to a photoprotective effect, which could extend to internal cellular components as melatonin is able to permeate membranes [7]. Melatonin's ability to permeate even the hemato-encephalic (blood–brain) barrier means that it is accessible to almost all somatic cells, further extending its potential influence and emphasizing the importance of understanding its interactions with cell membranes [7].

Sahin et al. investigated the effects of melatonin on membrane properties in multilamellar vesicles, and showed that the effects were strongly dependent on the melatonin concentration [12]. Previous studies by Severcan et al. have shown that in dehydrated DMPC model membranes, the addition of even a very small molar percentage of melatonin resulted in a phase separation within the membrane [13]. The inductance of a different phase has also been predicted by molecular dynamics simulations of membranes containing large amounts of

* Corresponding author at: Department of Physics and Astronomy, McMaster University, ABB-241, 1280 Main Street West, Hamilton, Ontario L8S 4 M1, Canada. Tel.: +1 905 525 9140 23134; fax: +1 905 546 1252.
E-mail addresses: dieshe@mcmaster.ca (H. Dies), rheinstadter@mcmaster.ca (M.C. Rheinstädter).

http://dx.doi.org/10.1016/j.bbamem.2015.01.006
0005-2736/

ethanol (also a small hydrophobic molecule which, similarly to melatonin, has been shown to increase membrane fluidity) [14].

Drolle et al. [6] used neutron diffraction and small angle scattering in combination with computer modelling to study the interaction between melatonin with bilayers made of DPPC and DOPC. The location of the melatonin molecules was determined at melatonin concentrations of ~10 mol% (in experiment and simulation) and ~30 mol% (in experiments). Melatonin was found to reside in the head group region of the bilayers and to lead to a decrease in bilayer thickness indicative of an increase of bilayer fluidity. Dies et al. [10] then presented experimental evidence that melatonin inhibits the insertion of amyloid-β_{25-35} peptides in anionic lipid membranes made of DMPC and DMPS at high melatonin concentrations of 30 mol%, which is considered to be an important step in protein oligomerization and toxic fibril formation. This observation supports the assumption of a potential protective role of melatonin in the formation of amyloid plaques in Alzheimer's disease.

In this study, we investigated the position and organization of melatonin in phospholipid membranes at different concentrations. This is achieved through the preparation of lipid membranes containing 1,2-dimyristoyl-sn-glycero-3-phosphatidylcholine (DMPC), a 14 chain saturated phospholipid with an overall zwitterionic nature, as shown in Fig. 1. Different amounts of melatonin ranging from 0.5 mol% to 30 mol% were included in the membranes. Using 2-dimensional X-ray diffraction, the in-plane and out-of-plane structure of the membranes was determined.

2. Results

Synthetic lipid membranes made of DMPC were prepared as highly oriented, multi-lamellar membrane stacks on silicon wafers. Lipids and melatonin at different concentrations were dissolved in a solvent and applied as thin films to the wafers. Five different membrane complexes were prepared for this study, as detailed in Section 5 and listed in Table 1. As depicted in Fig. 1b, the samples were oriented such that the $q_{||}$-axis probed lateral membrane structure and the perpendicular axis, q_z, probed out-of-plane structure of the multi-lamellar membrane complexes. The samples were kept in a temperature and humidity controlled chamber, a so-called humidity chamber, during the measurements. Data were collected at $T = 28$ °C and in a 100% H_2O atmosphere to ensure full hydration of the membranes to study structure in the fluid, physiologically relevant state of the membrane complexes.

Table 1
Molecular composition of all the samples prepared for this study and their structural parameters.

DMPC (mol%)	Melatonin (mol%)	d_{z1} (Å)	d_{z2} (Å)	d_{z3} (Å)	Lateral structure
100	0	66.17	–	–	
99.5	0.5	64.24	59.30	–	
99	1	61.63	59.30	48.18	
97.5	2.5	64.24	59.30	–	
95	5	65.89	55.06	–	
					$a_1 = 12.4$ Å, $b_1 = 10.1$ Å, $\gamma_1 = 90°$
70	30	66.17	–	–	$a_2 = 5.8$ Å, $b_2 = 5.3$ Å, $\gamma_2 = 98.5°$

Two-dimensional X-ray data are shown in Fig. 2. The data cover a large area of reciprocal space to determine the in-plane and out-of-plane structure of the membranes simultaneously. These maps are also important to identify potential scattering features from, e.g., molecular tilts, which may occur outside of the q_z and $q_{||}$ directions. The diffracted intensity shows one well developed in-plane Bragg peak along the $q_{||}$-axis at $q_{||} \sim 1.5$ Å^{-1}, related to the packing of the lipid acyl chains (with the exception of the 30 mol% melatonin sample, which will be discussed further in later sections). The intensity has a distinct rod-like shape, typical for a 2-dimensional system.

The out-of-plane scattering along q_z shows pronounced and equally spaced Bragg intensities due to the multi-lamellar structure of the membranes, as reviewed for instance in Refs. [15,16].

2.1. The low melatonin concentration membranes

For a quantitative analysis of the diffracted intensity, the 2-dimensional data were cut along the out-of-plane and in-plane axes.

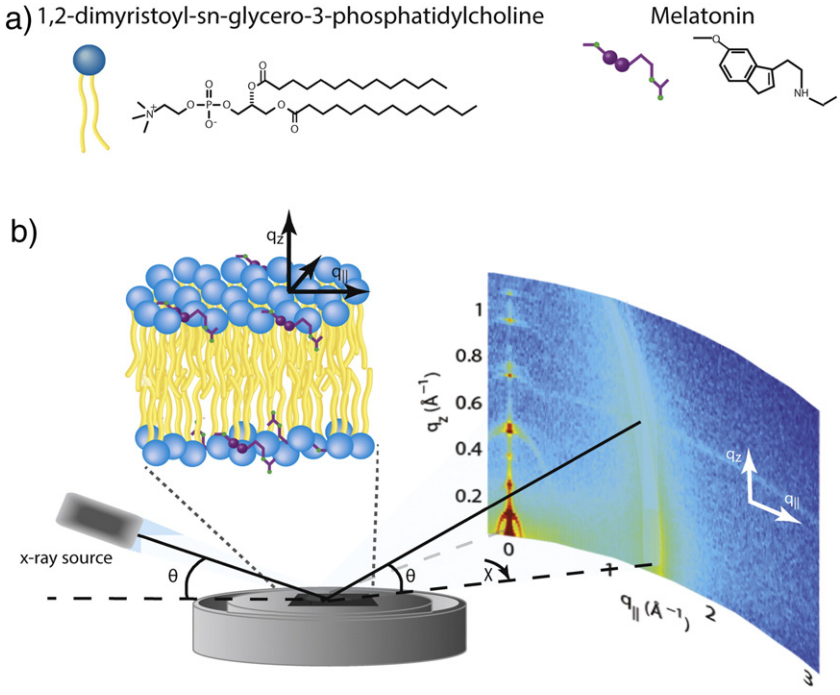

Fig. 1. (a) Schematic representations of DMPC and melatonin molecules. (b) Diagram of the experimental setup used for the X-ray diffraction measurements. Two-dimensional data sets were collected to study molecular structure perpendicular to the solid supported membranes (out-of-plane) and parallel to the membranes (in-plane). Abbreviations: DPPC — dipalmitoylphosphatidylcholine, DMPC — diymyristoylphosphatidylcholine, DMPS — dimyristoylphosphatidylserine, DB — Drug Bank, FWHM — full width half maximum, AFM — atomic force microcopy, FTIR — Fourier transform infrared spectroscopy, DCM, dichloromethane, TFE — trifluoroethanol, RH — relative humidity.

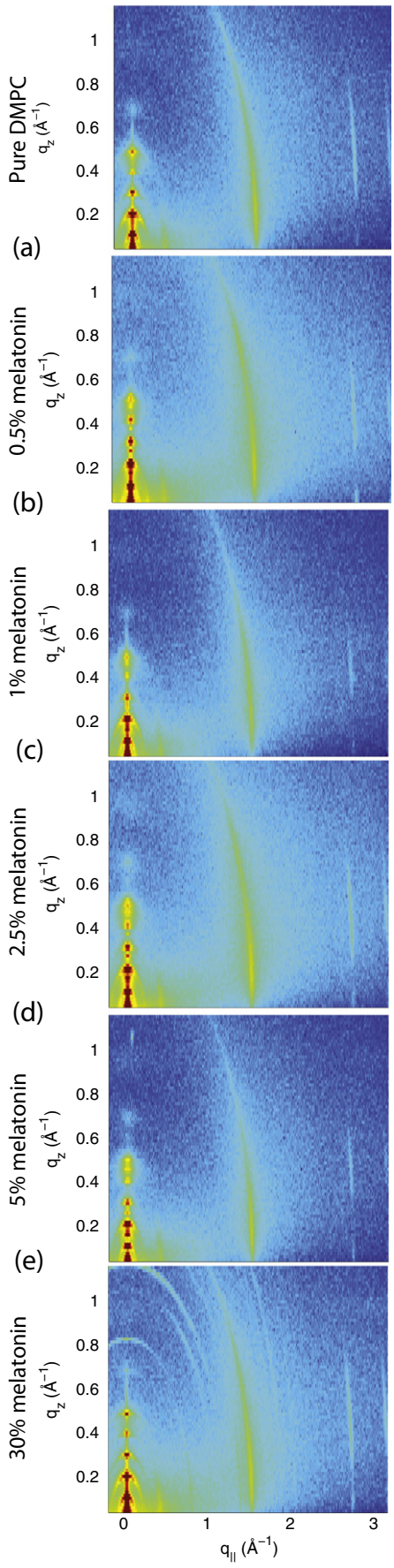

Fig. 2. Two-dimensional X-ray diffraction data for all samples prepared for the study, measured at 100% relative humidity, in the fluid phase of the membranes.

The corresponding reflectivities for pure DMPC, 2.5 mol% melatonin, and 30 mol% melatonin at 100% relative humidity are shown in Fig. 3a–c. Up to 8 diffraction orders were observed and used to construct the corresponding electron densities. The lamellar spacings, d_z, of the membrane complexes, i.e., the distance between two bilayers in the membrane stack, were determined from the positions of the Bragg peaks in the out-of-plane data, and are listed in Table 1.

As can be seen in Fig. 3b (and also in the 2-dimensional data in Fig. 2), the addition of melatonin to the saturated lipid bilayers leads to the appearance of additional Bragg reflections in the reflectivities. While splitting of peaks in X-ray reflectivity measurements generally

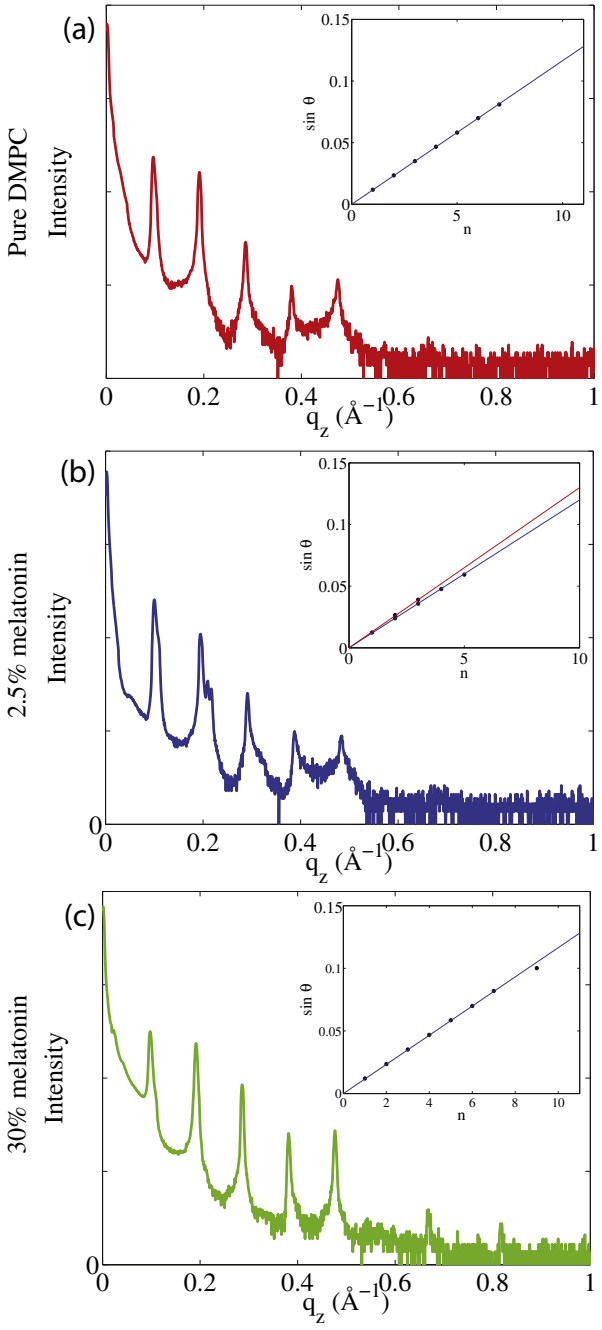

Fig. 3. X-ray reflectivity data at 100% RH. The peak positions ($\sin\theta$) are plotted vs. the peak indices to determine the d_z-spacing of different phases in the sample. (a) and (c) show pure DMPC and DMPC/30 mol% melatonin, respectively, both of which have uniform d_z-spacings throughout the sample. All other concentrations of melatonin ((b) is given as an example, with 2.5% melatonin), show peak splitting and multiple, coexisting phases.

complicates the data analysis, often resulting in disregard of these samples, we performed analysis on the reflectivity data with multiple split Bragg peaks in order to evaluate the d_z-spacings of the phase-separated regions in the lipid/melatonin bilayers.

To assign the peaks to different phases, Bragg's law can be re-written as $\sin(\theta) = \lambda/(2d_z)n$ (λ is the wavelength of the X-rays, 1.5418 Å). By plotting the sine of the Bragg angles versus the order of the different Bragg reflections, $\sin(\theta(n))$ vs. n, peaks which belong to the same d_z-spacing fall on a straight line through the origin, whose slope is proportional to $1/d_z$. The corresponding plots are shown as insets in Fig. 3 and the corresponding d_z-spacings listed in Table 1.

The dominant d_z-spacing, d_{z1}, of ~66 Å corresponds well with lamellar spacings reported for fully hydrated DMPC bilayers [17] and proves that the membranes were in their physiologically relevant fluid phase during the measurements. The second d_z-spacing (d_{z2} in Table 1) indicates a coexisting, smaller repeat distance in the presence of melatonin. We assigned this lamellar spacing to melatonin-enriched domains in the membranes.

The measured d_{z2}-spacing of the coexisting melatonin phase is, however, not directly equivalent to the thicknesses of the melatonin-enriched bilayer. There are three possibilities for arrangements of the domains in lamellar structures: (1) a lipid domain can be stacked on a lipid domain, (2) a lipid domain can be stacked on a melatonin-enriched domain, and (3) a melatonin-enriched domain can be stacked on another melatonin-enriched domain, as sketched in Fig. 4. The larger d_z-spacing was assigned to the distance between two lipid domains in the stack. This d_z-spacing is equivalent to the thickness of a bilayer including the water layer that separates neighbouring bilayers in the stack. The intermediate d_z-spacing (d_{z2}) involved a bilayer and an adjacent melatonin-enriched domain such that $d_{z2} = \frac{1}{2}d_{lipid} + \frac{1}{2}d_{mel}$. Finally, the smallest d_z-spacing (d_{z3}) directly corresponds to the melatonin-enriched domains. We note, however, that the likelihood of this situation is significantly smaller than for d_{z1} and d_{z3} as it critically depends on the number of melatonin-enriched domains, which is expected to be small at these small melatonin concentrations.

In order to investigate the structure of the melatonin-enriched domains, an electron density analysis was performed on a 2.5 mol% melatonin sample. This data was collected at 50% relative humidity, in a de-hydrated gel state of the lipid bilayers, to increase the number of higher order Bragg peaks and enhance structural features and achieve a high spatial resolution, as demonstrated for instance by Hristova and White [18]. The reflectivity for this sample is shown in Fig. 5a. The observed d_z-spacings of 53.35 Å and 46.72 Å are smaller than the d_z-spacings observed in the fluid membranes (see Table 1), as the membranes swell with hydration. However, in both cases two distinct phases are observed, with the melatonin-enriched phase being ~5–6 Å smaller than the melatonin phase, suggesting that the domain structure is preserved when de-hydrating the membrane stacks.

Fourier analyses of the peaks from the melatonin-enriched phase and the lipid phase were done separately, to yield electronic distributions for

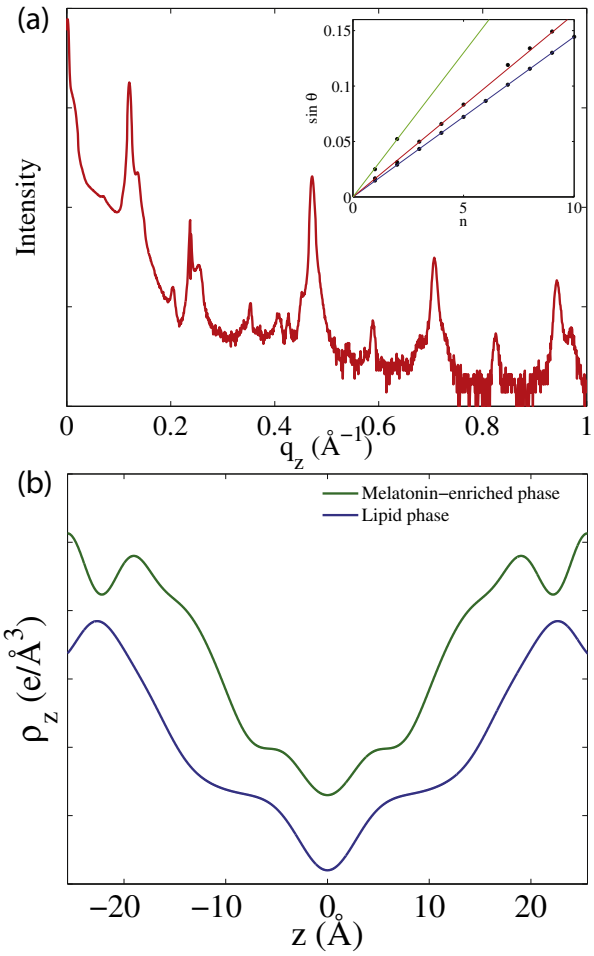

Fig. 5. Electron densities for a melatonin-enriched and a lipid phase in a 50% RH DMPC/2.5 mol% melatonin membrane. Relative electron densities are shown as the electron density at the centre of the membrane, as well as the molar percentages of melatonin in each domain are unknown.

these two separate domains. As shown in Fig. 5b, the melatonin-enriched phase has a smaller d_z-spacing, and a slightly increased electron density just below the head groups, at z values of $z \sim 15$ Å. Note that the scaling of these electronic densities is not absolute, as the exact percentage composition of melatonin in these domains was unknown, as well as the electron density at the centre of the head groups. From the overall shape of the electronic distribution, however, it is possible to develop a hypothesis for the structure of these melatonin domains.

The lipid phase involves gel-phase lipids with ordered tails and a larger d_z-spacing. The electron density of this phase, shown in Fig. 5b,

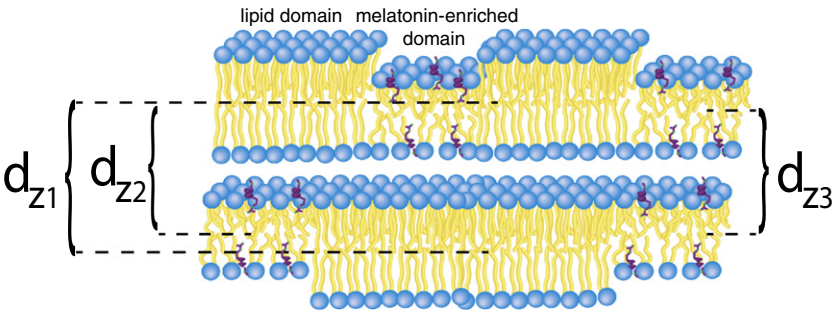

Fig. 4. Cartoon of a membrane containing small amounts of melatonin. The three d_z-spacings correspond to a melatonin-enriched phase, a lipid phase, and the repeated sequence of a melatonin-enriched phase in between two lipid phases.

agrees well with DMPC lipids in their gel state, as reported by Ref. [19]. As the electron density provides no evidence for the presence of melatonin molecules in these domains (within the resolution of this experiment), we denote this phase as a lipid phase. In the melatonin-enriched phase, there is an electron-dense region just below the lipid head groups.

In order to determine the melatonin position in the bilayers, DrugBank (DB) molecular structures of melatonin (DrugBank ID: 1065) were used to calculate 1-dimensional projections of the electron distributions along the *z*-axis of melatonin, as demonstrated in Ref. [10]. To take into account thermal motions of atoms and electrons, each atom was modelled by a Gaussian distribution with a width (FWHM) of 4 Å, and the corresponding electron distributions were summed. The result is plotted in Fig. 6. This analysis showed that the electronic distribution of melatonin can be well fit by two Gaussian distributions (Peak 1 and Peak 2 in Fig. 6). By subtracting those distributions from the electron density of the melatonin-enriched phase, the electron density of a pure gel-state DMPC membrane was obtained (see Fig. 7), suggesting that melatonin takes an upright configuration in these domains. We note that melatonin is approximately 15 Å in extent, such that it extends only partially the length of the lipid tails. Thus including melatonin in the membrane may result in a more fluid bilayer with a smaller d_z-spacing, in agreement with the experimental observations.

2.2. The high melatonin concentration membrane

At 30 mol% melatonin, additional diffraction patterns were observed in the in-plane diffraction data in Fig. 2e. A uniform d_z-spacing was observed, as can be seen in Fig. 3c, with $d_z \sim 66$ Å. Electron densities were obtained through Fourier transforms of the reflectivity peaks in Fig. 3c. The electron density of the pure DMPC membrane agrees well with electron densities reported for fluid DMPC membranes reported for instance by the Nagle group [17]. As shown in Fig. 8, the addition of 30 mol% melatonin significantly reduces the electron density in the membrane as electron-rich lipid molecules are replaced by less electron-dense melatonin molecules. By subtracting the electron density of the DMPC/30 mol% membrane from the pure lipid membrane, a difference profile was generated that was well fit by two Gaussian peaks, centred at *z*-values of $z = 12.8$ Å and 21.0 Å. The melatonin molecules were, therefore, found both slightly inside and slightly outside the lipid head groups in saturated bilayers made of DMPC. This position of melatonin is similar to the position reported for anionic lipid membranes by Dies et al. [10] and the Leonenko group [6,11] in DPPC/DOPC membranes. The absence of additional peaks in the reflectivity curve in Fig. 3c is indicative of a uniformly ordered distribution at high melatonin concentrations.

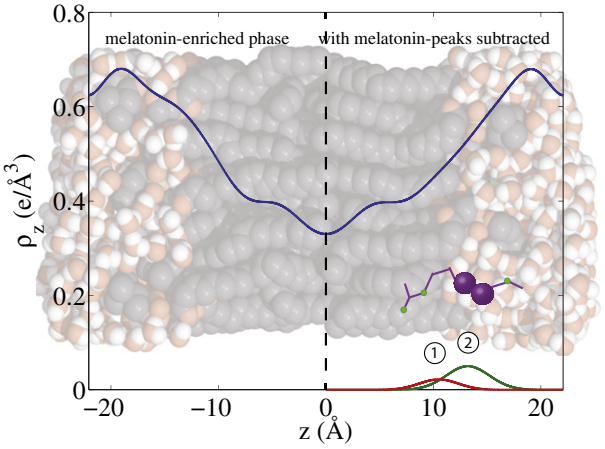

Fig. 7. The position of melatonin in a DMPC/2.5 mol% melatonin membrane domain. The left side shows the electron density for a melatonin-containing patch, and by subtracting Gaussian peaks labelled 1 and 2, the right side of the diagram can be generated, which agrees well with the electron density of a pure phospholipid membrane in its gel state.

2.3. Lateral membrane structure

The 2-dimensional X-ray data in Fig. 2 show well-defined peaks along the $q_{||}$-axis, which allow the determination of the lateral membrane structure. For a quantitative analysis, the diffracted intensity was radially integrated on the 2-dimensional X-ray data from $\phi = 30°$ to $\phi = 90°$. Results for DMPC, DMPC/2.5 mol% melatonin and DMPC/30 mol% melatonin are shown in Fig. 9. Several correlation peaks are observed in the in-plane data and were well fit by Lorentzian peak profiles. All samples containing less than 30 mol% melatonin showed one broad and one narrow Lorentzian peaks, centred at ~1.5 $Å^{-1}$ due to the organization of the lipid tails in the hydrophobic membrane core. The broad component is the tell-tale of a fluid membrane structure, where the lipid tails form a densely packed structure with hexagonal symmetry (planar group p6), as reported from, e.g., neutron diffraction [20]. The distance between two acyl chains is determined to be $a_T = 4\pi / \sqrt{3q_T}$

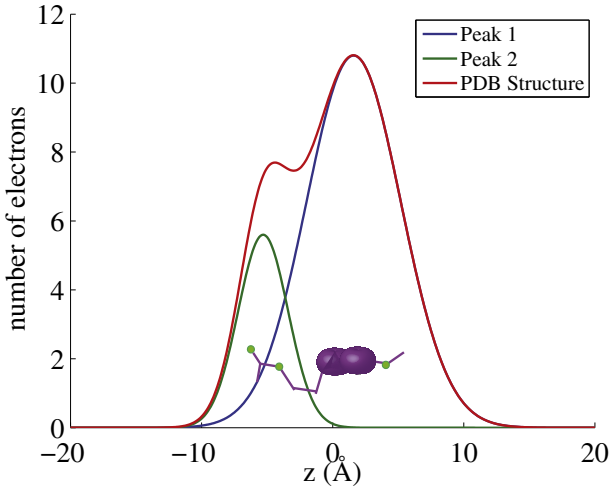

Fig. 6. The theoretical electron density of melatonin, obtained from DB structural information. Note that the distribution can be well fit by two Gaussian peaks, which agrees well with the experimentally observed electron density.

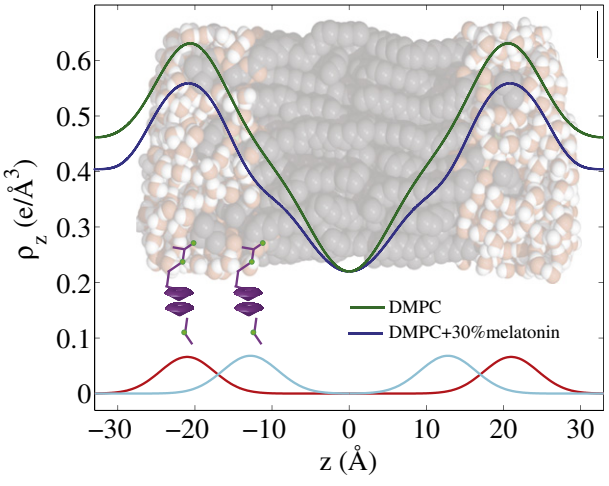

Fig. 8. Electron densities for a pure DMPC membrane as well as a membrane containing 30 mol% melatonin. The difference profile between the two distributions is well fit by two Gaussian peaks, shown along the bottom of the graph. Note that these are negative peaks, as melatonin reduces the number of electrons in the membrane.

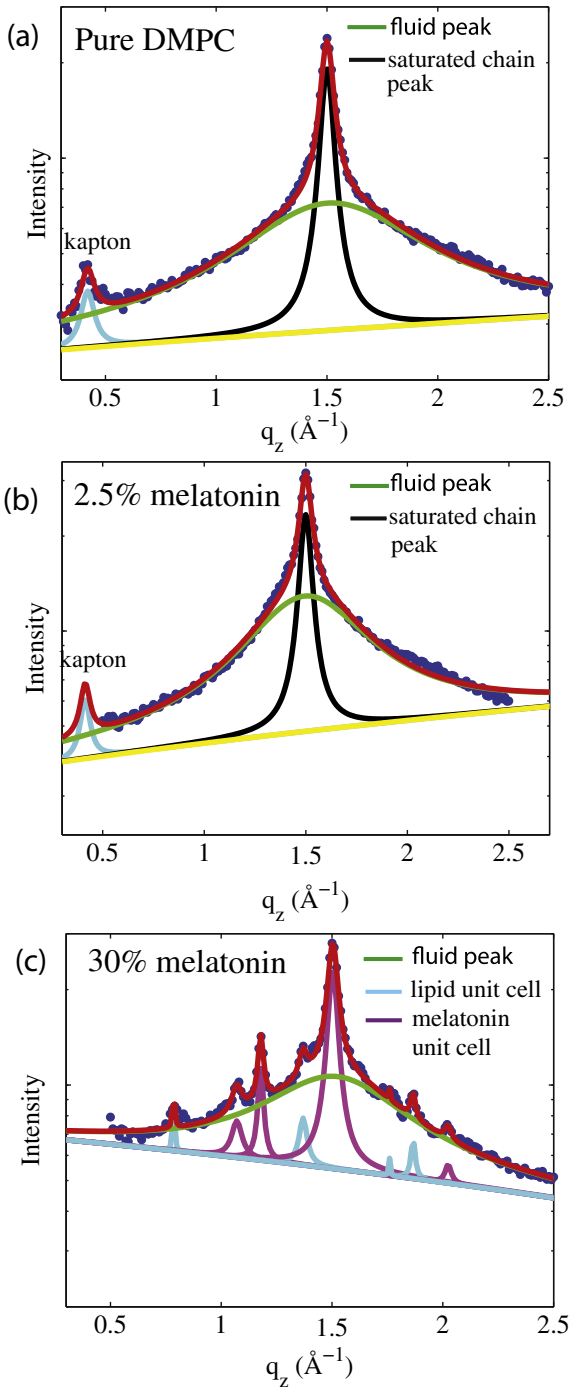

Fig. 9. Radial integrations to the 2-dimensional data for all samples used in the study, performed from $\phi = 30°$ to $\phi = 90°$. Peaks were well fit by Lorentzian peak profiles along with a linear background. (a) pure DMPC bilayers, (b) DMPC/2,5 mol% melatonin, and (c) DMPC/30 mol% melatonin. The peak at $q_{||} \sim 0.4$ Å^{-1} stems from the Kapton windows of the humidity chamber and was not included in the structure refinement.

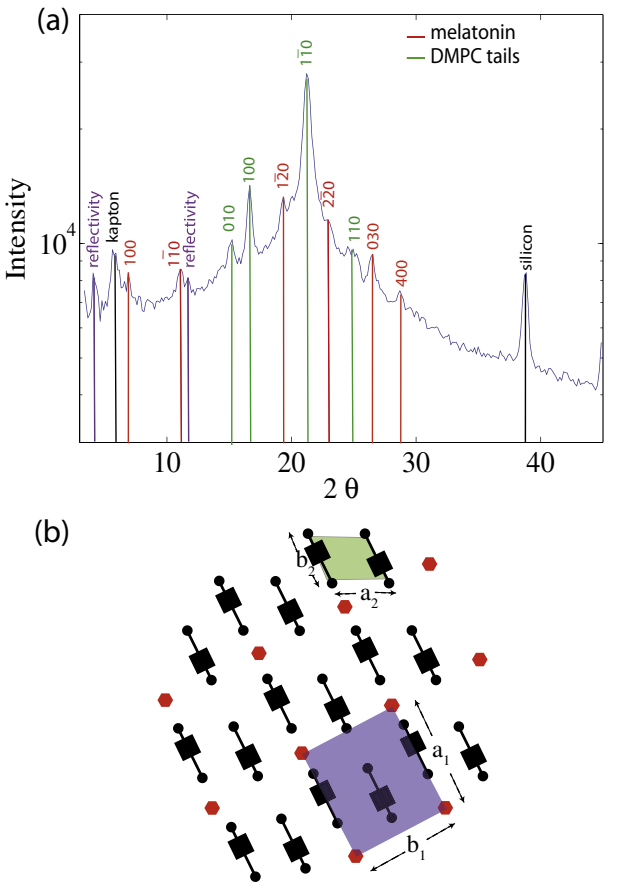

Fig. 10. (a) In-plane radially integrated intensity, plotted along with corresponding peaks determined from PowderCell fits. (b) Cartoon of a membrane containing melatonin. Lipids are represented by a head group (■) and two tails (●). Melatonin molecules are represented by a red hexagon. The peak pattern is well indexed by a superposition of an orthorhombic and a monoclinic lattice, as shown in the cartoon, with parameters $a_1 = 12.4$ Å, $b_1 = 10.1$ Å, $\gamma_1 = 90°$ and $a_2 = 5.8$ Å, $b_2 = 5.3$ Å, $\gamma_2 = 98.5°$. Peaks labelled by 'reflectivity' occur on the q_z-axis and were, therefore, excluded from the in-plane structure refinement.

with q_T being the position of the peak. As the broad component is centred at $q_{||} = 1.51$ Å^{-1}, the a_T is calculated at 4.16 Å. The narrow peak at $q_{||} = 1.50$ Å^{-1} is characteristic of the distance between saturated acyl chains (see, e.g., Ref [21] and references therein), with a distance of 4.19 Å.

Additional correlation peaks are observed at 30 mol% melatonin in Fig. 9c, indicative that lipid and melatonin molecules form a well ordered, crystal-like superstructure at this concentration (analogous to cholesterol or aspirin in-plane structures observed in Refs. [22,23]).

The resulting peak pattern is well indexed by a superposition of an orthorhombic lattice and a monoclinic lattice, as shown in Fig. 10a, with parameters $a_1 = 12.4$ Å, $b_1 = 10.1$ Å, $\gamma_1 = 90°$ and $a_2 = 5.8$ Å, $b_2 = 5.3$ Å, $\gamma_2 = 98.5°$. The larger rectangular lattice was assigned to the regular arrangement of melatonin molecules in the membrane, and the second, orthorhombic lattice was assigned to the organization of DMPC tails in the membrane. The resulting lateral membrane structure is depicted in the cartoon in Fig. 10b (the lattice constants are also given in Table 1). The melatonin molecules form a regular pattern, where each melatonin molecule is associated with 2 lipid molecules, in agreement with the molecular ratio of about 1:2 (melatonin:lipid molecules).

3. Discussion

Previous studies have identified that melatonin affects the dynamics of membranes in different ways at different concentrations; however, there is yet to be a structural explanation for these effects. For example, Garca et al. identified that melatonin reduces membrane rigidity in a manner that depends on the concentration. Sahin et al. showed that at low concentrations melatonin increases fluidity of lipids, at high concentrations it has the opposite effect [24].

Through 2-dimensional X-ray diffraction measurements, we present experimental evidence for two different regimes: (1) at low melatonin concentrations, melatonin forms fluid melatonin-enriched domains

coexisting with a pure lipid phase; and (2) at high melatonin concentrations, the melatonin molecules form an ordered structure uniform throughout the membrane. In the following section we discuss the structure of melatonin in membranes at high and low concentrations and develop structural evidence for these observed differences.

While melatonin concentrations in the blood are typically in the pico- to nanomolar range, melatonin concentrations in the cerebrospinal fluid in the brain were found to be orders of magnitude higher [25]. Experiments are typically conducted at higher melatonin concentrations in the order of millimolar concentrations [26]. The low melatonin concentrations in our study between 0.5 and 5 mol% correspond to concentrations of 0.1–1 mM, while 30 mol% melatonin corresponds to an elevated 10 mM concentration. We note that these concentrations are significantly higher than physiological concentrations, however, compare well with concentrations typically used in the literature.

3.1. Structure of low melatonin concentration membranes

We observed that in membranes containing from 0.5 mol% to 5 mol% melatonin, the melatonin formed fluid patches or domains within the membranes, with characteristic smaller d_z-spacings, coexisting with a pure lipid phase. This is in agreement with the work done by de Lima et al., who observed with atomic force microscopy (AFM) that melatonin membranes contain different lipid phase domains in solid-supported membranes [5]. They also studied the topology of membranes containing these domains and observed a non-uniform surface topology, likely corresponding to different d_z-spacings of these domains.

The position of the melatonin molecules in the melatonin-enriched and lipid patches was determined through Fourier analysis of the lipid and melatonin-enriched diffraction peaks, and electron density profiles for each of the two phases were generated and compared to calculated electron distributions based on DB structure files.

Within the melatonin-enriched patches, melatonin partitions in the membrane and aligns parallel to the phospholipid acyl chains, with the most electron dense region of the molecule located just below the hydrophilic head group region, at a z position of 13.2 Å, as depicted in Fig. 11a. This orientation is likely favourable in melatonin-enriched regions of the bilayer, as melatonin is an amphiphilic molecule, and this orientation allows it to minimize disruption to the lipid matrix. As the melatonin molecule is only ~15 Å in extent, it does not fully extend along the length of the lipid molecules, resulting in a thinning of the bilayers, most likely due to an increase in lipid tail fluctuations. This orientation is in agreement with observations from Akkas et al., who showed through FTIR that melatonin causes strengthening of hydrogen bonding in the hydrophilic zone along with disordering of the lipid tails in the hydrophobic zone [27].

The observation of small scale structure in lipid membranes is a highly discussed topic in membrane biophysics. Patches and plaques are often discussed in the presence of cholesterol ever since Simons and Ikonen [28] proposed the existence of so-called rafts in biological membranes. Rafts were thought to be small, molecularly organized units, providing local structure in fluid biological membranes and hence furnishing platforms for specific biological functions [20,22,28–40]. Rafts were supposed to be enriched in cholesterol making them more ordered, thicker and, thus, appropriate anchoring places for certain acylated and hydrophobically-matched integral membrane proteins. The existence of rafts is still highly debated in the literature as they were not established in cells [37,41,42], though experimental evidence for a heterogenous membrane structure in the presence of cholesterol was found recently in model membranes [20,39,40,43,44].

While rafts are generally interpreted as some kind of super-particles floating around in an otherwise structureless liquid membrane, lipid bilayers also show dynamic heterogeneities [45–48], driven by cooperative molecular interactions and thermal fluctuations that lead to density and compositional fluctuations in space and time. The observation of melatonin-enriched patches in the presence of moderate levels of melatonin is interesting, as patch or plaque formation was previously only discussed in association with cholesterol. While cholesterol generally leads to a stiffening of the bilayers, melatonin increases fluidity of membranes, most likely because of its different position in the head group region. The observation of patches now points to a potential interaction between melatonin molecules as driving force for the patch formation.

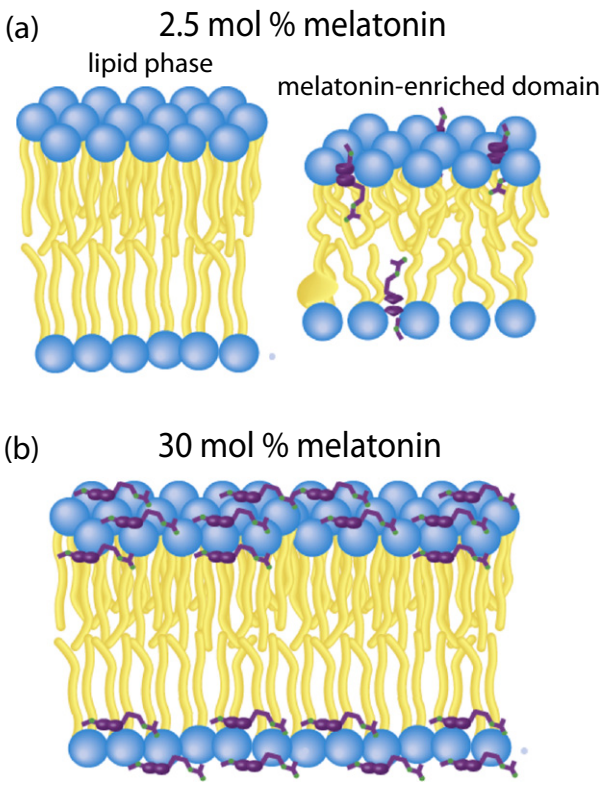

Fig. 11. a) At a concentration of 2.5 mol% melatonin, melatonin-enriched domains coexisting with a lipid phase are observed. The lipids in the lipid domains are in all-trans configuration with a large d_z-spacing. From the electron density in Fig. 7, the melatonin molecules align parallel to the lipid tails in these domains, with a smaller d_z-spacing. b) At 30 mol% melatonin, the electron density in Fig. 8 suggests that the melatonin molecules align parallel to the lipid membrane, in agreement with previous studies.

3.2. Structure of high melatonin concentration membranes

In membranes containing a high concentration of 30 mol% melatonin a single d_z-spacing was observed, indicative of a uniform membrane structure. Theoretically, each melatonin molecule can be associated with 2 lipid molecules at this concentration. The observation of a uniform membrane structure, without patches, is in agreement with a previous study by Dies et al. [10], using anionic lipid membrane made of DMPC/3 mol% DMPS. However, multiple in-plane peaks were observed at this concentration, suggesting an ordered lateral melatonin organization throughout the membrane. From analysis of these in-plane peaks, we suggest a lipid unit cell and a melatonin unit cell, which agree with the number of melatonin molecules per lipid in the membrane as well as the observed the X-ray diffraction peaks. The unit cells and the corresponding molecular structure are depicted in the cartoon in Fig. 10b.

The out-of-plane analysis of the high melatonin concentration membranes was used to determine the position of melatonin in the membranes. At a concentration of 30 mol%, the melatonin molecules are located in the head group region of the membranes and align parallel to the lipid bilayers, as shown in Fig. 11b. This position is in

agreement with observations from Drolle et al. [9] and Choi et al. [11] for DPPC bilayers containing 9 mol% melatonin, as well as from Severcan et al. [13] for DPPC bilayers containing 24 and 30 mol% melatonin and Dies et al. for anionic DMPC/DMPS membranes [10]. From our in-plane data we conclude that each melatonin molecule is then associated with 2 lipid molecule at this concentration.

4. Conclusions

In summary, we studied the in-plane and out-of-plane structures of phospholipid membranes containing melatonin at concentrations between 0.5 mol% and 30 mol% in their physiologically relevant fluid phase using high resolution X-ray diffraction. At low melatonin concentrations, small melatonin-enriched domains with smaller membrane thicknesses were observed. By comparing experimentally determined electron density profiles of the melatonin-enriched patches with calculations of the electron distribution of melatonin structures from the drug database, the melatonin molecules were found to penetrate the bilayers and align parallel to the lipid acyl chains in these patches.

Conversely, at a high melatonin concentrations of 30 mol%, a uniform distribution of melatonin throughout the membrane was observed, where the melatonin molecules align parallel to the membranes. From 2-dimensional X-ray diffraction, we present evidence that the melatonin molecules organize in a crystal-like structure in the membrane plane with orthorhombic symmetry, where one melatonin molecule associates with two lipid molecules. Understanding the interaction and organization of melatonin in biological membranes is an essential step towards deciphering its mechanism of influence on the membrane and its potential protective abilities.

5. Materials and methods

5.1. Preparation of the highly-oriented multi-lamellar membrane samples

Highly oriented multi-lamellar membranes were prepared on single-side polished silicon wafers. 100 mm diameter, 300 μm thick silicon (100) wafers were pre-cut into 1 × 1 cm^2 chips. The wafers were first pretreated by sonication in dichloromethane (DCM) at 310 K for 25 min to remove all organic contamination and leave the substrates in a hydrophilic state. Each wafer was thoroughly rinsed three times by alternating with ~50 mL of ultrapure water and methanol.

Individual solutions of 1,2-dimyristoyl-sn-glycero-3-phosphocholine (DMPC) and melatonin (depicted in Fig. 1a) were each dissolved in 1:1 chloroform:2,2,2-trifluoroethanol (TFE). The DMPC and melatonin solutions were then mixed in appropriate ratios to produce the desired membrane samples for the experiment.

A tilting incubator was heated to 313 K and the lipid solutions were placed inside to equilibrate. 65 μL of lipid solution was applied on each wafer, and the solvent was then allowed to slowly evaporate for 10 min at a speed of 15, tilt of 1, such that the lipid solution spreads evenly on the wafers. After drying, the samples were placed in vacuum at 313 K for 12 h to remove all traces of the solvent. The bilayers were annealed and rehydrated before use in a saturated K_2SO_4 solution which provides ~98% relative humidity (RH). The hydration container was allowed to equilibrate at 293 K in an incubator. The temperature of the incubator was then increased gradually from 293 K to 303 K over a period of ~5 h to slowly anneal the multi-lamellar structure. This procedure results in highly oriented multi-lamellar membrane stacks and a uniform coverage of the silicon substrates. About 3000 highly oriented stacked membranes with a thickness of ~10 μm are produced using this protocol.

5.2. X-ray scattering experiment

Out-of-plane and in-plane X-ray scattering data was obtained using the Biological Large Angle Diffraction Experiment (BLADE) in the Laboratory for Membrane and Protein Dynamics at McMaster University. BLADE uses a 9 kW (45 kV, 200 mA) CuK-α Rigaku Smartlab rotating anode at a wavelength of 1.5418 Å. Both source and detector are mounted on movable arms such that the membranes stay horizontal during the measurements. Focussing multi-layer optics provide a high intensity parallel beam with monochromatic X-ray intensities up to 10^{10} counts/(s × mm^2). This beam geometry provides optimal illumination of the solid supported membrane samples to maximize the scattering signal. A sketch of the scattering geometry is shown in Fig. 1c. By using highly oriented membrane stacks, the in-plane ($q_{||}$) and out-of-plane (q_z) structure of the membranes could be determined. From the high resolution X-ray diffraction experiments we determine the molecular structure of the membranes in two different ways: (1) the out-of-plane membrane structure to determine the location of the different molecules in the membrane with sub-nanometre resolution and (2) the lateral organization of the different molecular components in the plane of the membrane. The result of such an X-ray experiment is a 2-dimensional intensity map of a large area (0.03 $Å^{-1} < q_z < 1.1$ $Å^{-1}$ and 0 $Å^{-1} < q_{||} < 3.1$ $Å^{-1}$) of the reciprocal space.

5.3. Out-of-plane structure and electron densities

The out-of-plane structure of the membranes was determined using specular reflectivity, see, e.g., [15,16,23]. The electron density, $p(z)$, is approximated by a 1-dimensional Fourier analysis [19]:

$$\begin{aligned}\rho(z) &= \rho_W + \frac{F(0)}{d_z} + \frac{2}{d_z}\sum_{n=1}^{N} F(q_n)\nu_n \cos(q_n z) \\ &= \rho_W + \frac{F(0)}{d_z} + \frac{2}{d_z}\sum_{n=1}^{N} \sqrt{I_n q_n}\,\nu_n \cos\left(\frac{2\pi n z}{d_z}\right).\end{aligned} \quad (1)$$

N is the in the experiment and ρ_W the electron density of bulk water. The integrated peak intensities, I_n, are multiplied by q_n to receive the form factors, $F(q_n)$ [49,50]. The bilayer form factor $F(q_z)$, which is in general a complex quantity, is real-valued in the case of centro-symmetry. The phase problem of crystallography, therefore, simplifies to the sign problem $F(q_z) = \pm |F(q_z)|$. and the phases, ν_n, can only take the values ± 1. The phases ν_n are needed to reconstruct the electron density profile from the scattering data following Eq. (1). When the membrane form factor $F(q_z)$ is measured at several q_z values, a continuous function, $T(q_z)$, which is proportional to $F(q_z)$, can be fitted to the data [49–52]:

$$T(q_z) = \sum_n \sqrt{I_n q_n}\,\mathrm{sinc}\left(\frac{1}{2} d_z q_z - \pi n\right). \quad (2)$$

Once an analytical expression for $T(q_z)$ has been determined from fitting the experimental peak intensities, the phases ν_n can be assessed from $T(q_z)$.

In order to put p_z on an absolute scale, the electron densities were scaled to fulfil the condition $p(0) = 0.22$ e/$Å^3$ (the electron density of a CH_3 group) in the centre of the bilayer. Rather than normalizing $p(d_z/2)$ (the electron density at the surface of the bilayer) to that of water, the electron densities were scaled such that the integral of the electron density across the bilayer, multiplied by the area per lipid yielded the required number of electrons. This method of normalization was advantageous due to the fact that most samples contained melatonin, a molecule which has previously been hypothesized to position in the head group region.

The d_z-spacing between two neighbouring membranes in the stack was determined from the distance between the well developed Bragg reflections ($d_z = 2\pi/\Delta q_z$) along the out-of-plane axis, q_z. The peaks were well fit by Gaussian peak profiles. To assign the peaks to different phases, Bragg's law can be re-written as $\sin(\theta) = \lambda/(2d_z) \times n$. By plotting the sine of the Bragg angles versus the order of the different Bragg reflections, $\sin(\theta(n))$ vs. n, peaks which belong to the same d_z-spacing fall on a straight line through the origin, whose slope is

proportional to $1/d_z$. Up to a peak order n of 10 was observed in the out-of-plane data. Note that not all diffraction orders are necessarily observed for the d_z-spacings as their scattering intensity depends on the form factor of the bilayers and oscillates between zero and maximum intensity as a function of q_z.

Transparency document

The Transparency document associated with this article can be found, in the online version.

Acknowledgements

This research was funded by the Natural Sciences and Engineering Research Council of Canada (NSERC), the National Research Council Canada (NRC), the Canada Foundation for Innovation (CFI) and the Ontario Ministry of Economic Development and Innovation. H.D. and J.T. are recipients of NSERC Undergraduate Research Awards (USRA), M.C.R. is the recipient of an Early Researcher Award of the Province of Ontario.

References

[1] F.R. Maxfield, I. Tabas, Role of cholesterol and lipid organization in disease, Nature 438 (2005) 612–621.
[2] D. Acuña-Castroviejo, G. Escames, C. Venegas, M.E. Daz-Casado, E. Lima-Cabello, et al., Extrapineal melatonin: sources, regulation, and potential functions, Cell. Mol. Life Sci. 1–29 (2014).
[3] S. Tengattini, R.J. Reiter, D.X. Tan, M.P. Terron, L.F. Rodella, et al., Cardiovascular diseases: protective effects of melatonin, J. Pineal Res. 44 (2008) 16–25.
[4] M.A. Pappolla, M. Sos, R.A. Omar, R.J. Bick, D.L. Hickson-Bick, et al., Melatonin prevents death of neuroblastoma cells exposed to the Alzheimer amyloid peptide, J. Neurosci. 17 (1997) 1683–1690.
[5] V.R. De Lima, M.S. Caro, M.L. Munford, B. Desbat, E. Dufourc, et al., Influence of melatonin on the order of phosphatidylcholine-based membranes, J. Pineal Res. 49 (2010) 169–175.
[6] E. Drolle, N. Kučerka, M. Hoopes, Y. Choi, J. Katsaras, et al., Effect of melatonin and cholesterol on the structure of DOPC and DPPC membranes, Biochim. Biophys. Acta Biomembr. 1828 (2013) 22472254.
[7] A. Saija, A. Tomaino, D. Trombetta, M.L. Pellegrino, B. Tita, et al., Interaction of melatonin with model membranes and possible implications in its photoprotective activity, Eur. J. Pharm. Biopharm. 53 (2002) 209–215.
[8] A. Choucair, M. Chakrapani, B. Chakravarthy, J. Katsaras, L. Johnston, Preferential accumulation of aβ (1–42) on gel phase domains of lipid bilayers: an AFM and fluorescence study, Biochim. Biophys. Acta Biomembr. 1768 (2007) 146–154.
[9] E. Drolle, R.M. Gaikwad, Z. Leonenko, Nanoscale electrostatic domains in cholesterol-laden lipid membranes create a target for amyloid binding, Biophys. J. 103 (2012) L27–L29.
[10] H. Dies, L. Toppozini, M. Rheinstädter, The interaction between amyloid-β peptides and anionic lipid membranes containing cholesterol and melatonin, PLoS ONE 9 (2014) e99124.
[11] Y. Choi, S.J. Attwood, M.I. Hoopes, E. Drolle, M. Karttunen, et al., Melatonin directly interacts with cholesterol and alleviates cholesterol effects in dipalmitoylphosphatidylcholine monolayers, Soft Matter 10 (2014) 206–213.
[12] I. Sahin, F. Severcan, N. Kazanc, Melatonin induces opposite effects on order and dynamics of anionic DPPG model membranes, J. Mol. Struct. 834 (2007) 195–201.
[13] F. Severcan, I. Sahin, N. Kazanc, Melatonin strongly interacts with zwitterionic model membranes evidence from Fourier transform infrared spectroscopy and differential scanning calorimetry, Biochim. Biophys. Acta Biomembr. 1668 (2005) 215–222.
[14] M. Kranenburg, M. Vlaar, B. Smit, Simulating induced interdigitation in membranes, Biophys. J. 87 (2004) 1596–1605.
[15] G. Pabst, N. Kučerka, M.P. Nieh, M. Rheinstädter, J. Katsaras, Applications of neutron and x-ray scattering to the study of biologically relevant model membranes, Chem. Phys. Lipids 163 (2010) 460–479.
[16] G. Fragneto, M. Rheinstädter, Structural and dynamical studies from bio-mimetic systems: an overview, Compt. Rendus Phys. 8 (2007) 865–883.
[17] N. Kučerka, Y. Liu, N. Chu, H.I. Petrache, S. Tristram-Nagle, et al., Structure of fully hydrated fluid phase DMPC and DLPC lipid bilayers using x-ray scattering from oriented multilamellar arrays and from unilamellar vesicles, Biophys. J. 88 (2005) 2626–2637.
[18] K. Hristova, S.H. White, Determination of the hydrocarbon core structure of fluid dioleoylphosphocholine (DOPC) bilayers by x-ray diffraction using specific bromination of the double-bonds: effect of hydration, Biophys. J. 74 (1998) 2419–2433.
[19] S. Tristram-Nagle, Y. Liu, J. Legleiter, J.F. Nagle, Structure of gel phase DMPC determined by x-ray diffraction, Biophys. J. 83 (2002) 3324–3335.
[20] C.L. Armstrong, D. Marquardt, H. Dies, N. Kučerka, Z. Yamani, et al., The observation of highly ordered domains in membranes with cholesterol, PLoS ONE 8 (2013) e66162.
[21] D. Poinapen, L. Toppozini, H. Dies, D.C.W. Brown, M.C. Rheinstädter, Static magnetic fields enhance lipid order in native plant plasma membrane, Soft Matter 9 (2013) 6804–6813.
[22] M. Barrett, S. Zheng, L. Toppozini, R. Alsop, H. Dies, et al., Solubility of cholesterol in lipid membranes and the formation of immiscible cholesterol plaques at high cholesterol concentrations, Soft Matter 9 (2013) 9342–9351.
[23] M.A. Barrett, S. Zheng, G. Roshankar, R.J. Alsop, R.K. Belanger, et al., Interaction of aspirin (acetylsalicylic acid) with lipid membranes, PLoS ONE 7 (2012) e34357.
[24] J.J. Garcìa, R.J. Reiter, J.M. Guerrero, G. Escames, B.P. Yu, et al., Melatonin prevents changes in microsomal membrane fluidity during induced lipid peroxidation, FEBS Lett. 408 (1997) 297–300.
[25] R.J. Reiter, D.X. Tan, What constitutes a physiological concentration of melatonin? J. Pineal Res. 34 (2003) 79–80.
[26] D. Pozo, R.J. Reiter, J.R. Calvo, J.M. Guerrero, Physiological concentrations of melatonin inhibit nitric oxide synthase in rat cerebellum, Life Sci. 55 (1994) PL455–PL460.
[27] S.B. Akkas, S. Inci, F. Zorlu, F. Severcan, Melatonin affects the order, dynamics and hydration of brain membrane lipids, J. Mol. Struct. 834 (2007) 207–215.
[28] K. Simons, E. Ikonen, Functional rafts in cell membranes, Nature 387 (1997) 569572.
[29] K. Simons, E. Ikonen, How cells handle cholesterol, Science 290 (2000) 1721–1726.
[30] D.M. Engelman, Membranes are more mosaic than fluid, Nature 438 (2005) 578–580.
[31] P.S. Niemelä, S. Ollila, M.T. Hyvnen, M. Karttunen, I. Vattulainen, Assessing the nature of lipid raft membranes, PLoS Comput. Biol. 3 (2007) e34.
[32] L.J. Pike, The challenge of lipid rafts, J. Lipid Res. 50 (2009) S323–S328.
[33] D. Lingwood, K. Simons, Lipid rafts as a membrane-organizing principle, Science 327 (2010) 46–50.
[34] C. Eggeling, C. Ringemann, R. Medda, G. Schwarzmann, K. Sandhoff, et al., Direct observation of the nanoscale dynamics of membrane lipids in a living cell, Nature 457 (2009) 1159–1162.
[35] F.G. van der Goot, T. Harder, Raft membrane domains: from a liquid-ordered membrane phase to a site of pathogen attack, Semin. Immunol. 13 (2001) 89–97.
[36] P.F. Lenne, A. Nicolas, Physics puzzles on membrane domains posed by cell biology, Soft Matter 5 (2009) 2841–2848.
[37] K. Simons, M.J. Gerl, Revitalizing membrane rafts: new tools and insights, Nat. Rev. Mol. Cell Biol. 11 (2010) 688–699.
[38] R.J. Alsop, M.A. Barrett, S. Zheng, H. Dies, M.C. Rheinstädter, Acetylsalicylic acid (ASA) increases the solubility of cholesterol when incorporated in lipid membranes, Soft Matter 10 (2014) 4275–4286.
[39] R.J. Alsop, L. Toppozini, D. Marquardt, N. Kučerka, T.A. Harroun, et al., Aspirin inhibits formation of cholesterol rafts in fluid lipid membranes, Biochim. Biophys. Acta Biomembr. 1848 (2015) 805–812.
[40] L. Toppozini, S. Meinhardt, C.L. Armstrong, Z. Yamani, N. Kučerka, et al., Structure of cholesterol in lipid rafts, Phys. Rev. Lett. 113 (2014) 228101.
[41] O.G. Mouritsen, The liquid-ordered state comes of age, Biochim. Biophys. Acta Biomembr. 1798 (2010) 1286–1288.
[42] M.C. Rheinstädter, O.G. Mouritsen, Small-scale structures in fluid cholesterol-lipid bilayers, Curr. Opin. Colloid Interface Sci. 18 (2013) 440–447.
[43] C.L. Armstrong, M.A. Barrett, A. Hiess, T. Salditt, J. Katsaras, et al., Effect of cholesterol on the lateral nanoscale dynamics of fluid membranes, Eur. Biophys. J. 41 (2012) 901–913.
[44] C.L. Armstrong, W. Häußler, T. Seydel, J. Katsaras, M.C. Rheinstädter, Nanosecond lipid dynamics in membranes containing cholesterol, Soft Matter 10 (2014) 2600–2611.
[45] A. Dibble, A.K. Hinderliter, J.J. Sando, R.L. Biltonen, Lipid lateral heterogeneity in phosphatidylcholine/phosphatidylserine/diacylglycerol vesicles and its influence on protein kinase c activation, Biophys. J. 71 (1996) 1877–1890.
[46] O.G. Mouritsen, R.L. Biltonen, Protein–lipid interactions and membrane heterogeneity, New Compr. Biochem. 25 (1993) 1–39.
[47] O.G. Mouritsen, K. Jørgensen, Dynamical order and disorder in lipid bilayers, Chem. Phys. Lipids 73 (1994) 3–25.
[48] O.G. Mouritsen, K. Jørgensen, Small-scale lipid–membrane structure: simulation versus experiment, Curr. Opin. Struct. Biol. 7 (1997) 518–527.
[49] J.F. Nagle, M.C. Wiener, Relations for lipid bilayers, Biophys. J. 55 (1989) 309–313.
[50] J. Nagle, R. Zhang, S. Tristram-Nagle, W. Sun, H. Petrache, et al., X-ray structure determination of fully hydrated lα phase dipalmitoylphosphatidylcholine bilayers, Biophys. J. 70 (1996) 1419–1431.
[51] G.I. King, C.R. Worthington, Analytic continuation as a method of phase determination, Phys. Lett. 35A (1971) 259–260.
[52] T. Adachi, A new method for determining the phase in the x-ray diffraction structure analysis of phosphatidylcholine:alcohol, Chem. Phys. Lipids 107 (2000) 93–97.